IOPscience iopscience.iop.org

Home Search Collections Journals About Contact us My IOPscience

Atomic-scale characterization of (mostly zincblende) compound semiconductor heterostructures

This content has been downloaded from IOPscience. Please scroll down to see the full text.

2013 J. Phys.: Conf. Ser. 471 012005

(http://iopscience.iop.org/1742-6596/471/1/012005)

View the table of contents for this issue, or go to the journal homepage for more

Download details:

IP Address: 209.147.144.22
This content was downloaded on 03/02/2015 at 17:07

Please note that terms and conditions apply.

Atomic-scale characterization of (mostly zincblende) compound semiconductor heterostructures

David J Smith[1,2], T Aoki[3], J K Furdyna[4], X Liu[4], M R McCartney[1,2] and Y-H Zhang[2,5]

[1] Department of Physics, Arizona State University, Tempe, AZ 85287, USA
[2] Center for Photonics Innovation, Arizona State University, Tempe, AZ 85287, USA
[3] LeRoy Eyring Center for Solid State Science, Arizona State University, Tempe, AZ 85287, USA
[4] Department of Physics, University of Notre Dame, Notre Dame, IN 46556, USA
[5] School of Electrical, Computer and Energy Engineering, Arizona State University, Tempe, AZ 85287, USA

E-mail: david.smith@asu.edu

Abstract. This paper provides an overview of our recent atomic-scale studies of semiconductor heterostructures, based primarily on combinations of zincblende compound materials grown by molecular beam epitaxy. Interfacial strain due to lattice mismatch inevitably causes growth defects to be introduced. Analysis of defect type and distribution using image filtering allows residual strain to be estimated. Exploratory investigations using aberration-corrected electron microscopy, which enables individual atomic columns to be resolved, are also described.

1. Introduction

Compound semiconductors offer a multitude of optoelectronic and photonic device opportunities based on their wide range of band gaps that cover wavelengths from far-infrared to near-ultraviolet. These possibilities are illustrated in Fig. 1, which depicts the lattice constants and band-gap energies of many common semiconductors [1]. Ternary (and quaternary) alloys offer additional flexibility in terms of band-gap engineering, as well as potentially allowing for avoidance of any lattice-mismatch issues. Nevertheless, the epitaxial growth of compound semiconductor heterostructures with two (or more) dissimilar materials presents many challenges. Successful growth requires suitable preparation of the substrate surface and careful attention to the growth conditions. For materials with differing lattice parameters, there are several additional problems. As well as lattice mismatch, which inevitably leads to strain and probable defect formation, valence mismatch and differences in thermal expansion are further factors that can seriously impact whether or not high quality materials can be grown.

The transmission electron microscope (TEM) provides a wide range of techniques for structural characterization of compound semiconductors including high-resolution electron microscopy (defect identification and strain field analysis), Z-contrast imaging (cation distribution), convergent-beam electron diffraction (local lattice parameter), and electron holography (internal electric field). These TEM methods provide powerful complementary approaches for characterizing and understanding the often-competing effects of growth conditions and compositional differences. In the following, we briefly review our recent atomic-scale investigations of heterostructures consisting of II-VI compound semiconductors grown epitaxially on several common III-V substrates.

Content from this work may be used under the terms of the Creative Commons Attribution 3.0 licence. Any further distribution of this work must maintain attribution to the author(s) and the title of the work, journal citation and DOI.
Published under licence by IOP Publishing Ltd

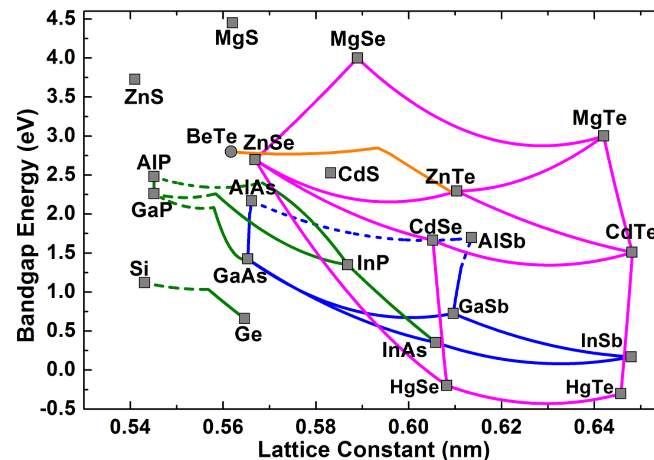

Figure 1. Schematic showing band gaps of common semiconductors vs. corresponding lattice parameter.

2. Experimental details

Most of the heterostructures described here were grown by molecular beam epitaxy (MBE), as described elsewhere [2], using a Riber 32 system consisting of two separate III-V and II-VI chambers connected via an ultrahigh-vacuum transfer module. The different III-V substrates were normally deoxidized, followed by growth of a thin buffer layer of the same material (except in the case of InP), before being cooled down to room temperature and then transferred to the II-VI chamber. Monitoring of the II-VI surface reconstruction during growth using reflection-high-energy electron diffraction (RHEED) was used to maintain optimal deposition conditions.

Samples were prepared for cross-sectional TEM observation using standard mechanical polishing and dimpling to reduce sample thicknesses to ~10μm, followed by argon-ion-milling at low energy (~2.0-3.0keV) with the sample held at liquid-nitrogen temperature to minimize ion-beam damage [3]. All samples were prepared for observation along [110]-type zone axes so that the interface normal would be perpendicular to the electron-beam direction [4]. The observations described here were made either with a JEM-4000EX high-resolution electron microscope (HREM) operated at 400keV (structural resolution of ~1.7Å), or a probe-corrected JEM-ARM200F scanning TEM (STEM) operated at 200keV (probe size ~0.8Å). Images from the latter instrument were primarily recorded using high-angle annular-dark-field (HAADF) and/or bright-field (BF) imaging modes, with corresponding detector collection angles of ~90-170mrad and ~0-22mrad, respectively.

3. Results

3.1. High-resolution lattice-fringe imaging

The characterization of zincblende compound semiconductors by electron microscopy methods has attracted much attention over several decades. Here we illustrate some recent developments by comparing changes in the microstructure of epitaxial ZnTe layers as a function of lattice mismatch with the underlying substrate material, focusing primarily on the stress-relieving defects that are present at the hetero-interfaces. Projections of individual atomic columns are clearly resolved in probe-corrected HAADF and BF images, as will be shown below.

In the case of the ZnTe(001)/GaSb(001) heterostructure, where the lattice mismatch was ~0.13%, misfit dislocations were occasionally visible at the interface but they were usually highly separated (>0.1μm apart). Moreover, the exact position of the interface was otherwise difficult to determine except in some diffraction contrast images, which was ascribed to the close similarity in the combined atomic numbers of the two elements in each material [3]. Similar results were also obtained in related studies of ZnTe(211)/GaSb(211)B heterostructures, as shown by the example in Fig. 2 [5].

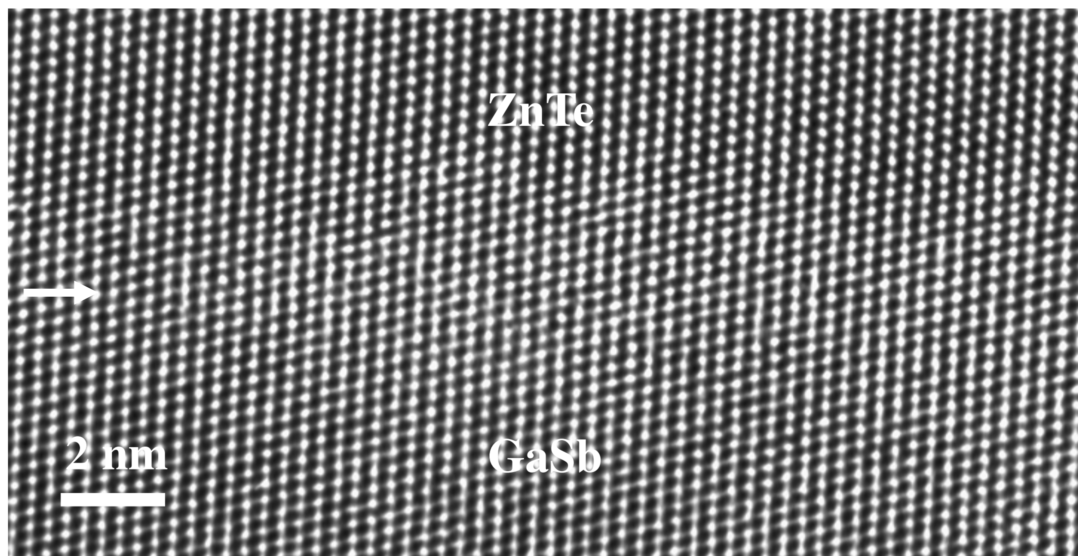

Figure 2. High-resolution electron micrograph establishing the highly coherent nature of the ZnTe(211)/GaSb(211)B interface (arrowed). Black spots correspond to closely-spaced pairs of atomic columns that are not separately resolved [5].

For the ZnTe(001)/InAs(001) sample, where the lattice mismatch between the two materials was slightly larger (~0.74%), threading dislocations were observed in the thick ZnTe epilayer and some strain-related contrast at the interface was also visible in diffraction-contrast images [6]. However, as shown by the lattice-fringe image in Fig. 3, the ZnTe/GaAs interface was invariably abrupt and coherent although its exact position was difficult to recognize.

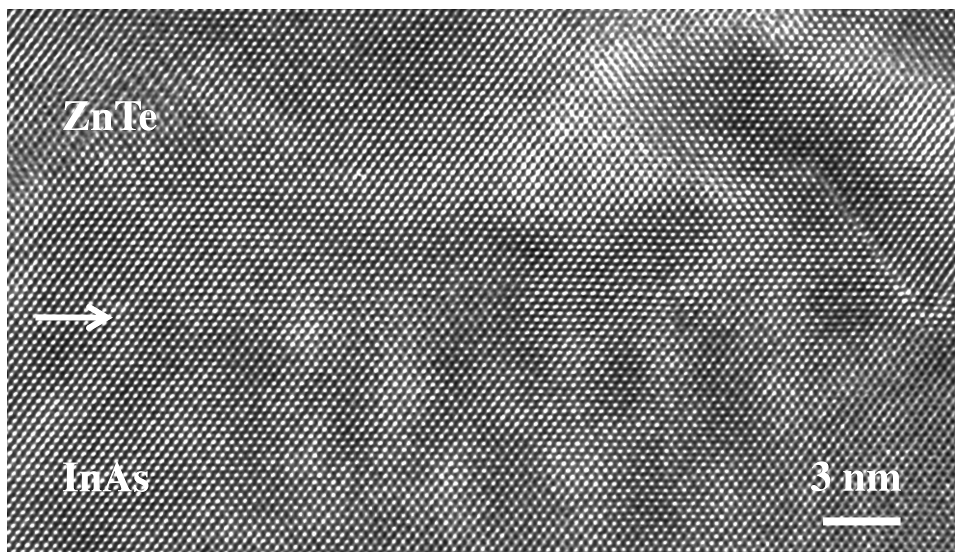

Figure 3. High-resolution lattice-fringe image of ZnTe/InAs(001) interface. The location of the interface (arrowed) is almost impossible to identify in the absence of misfit dislocations.

The interfacial defect density increased substantially as the difference in lattice parameters was increased. In the case of the ZnTe(001)/InP(001) sample (lattice mismatch ~3.85%), Burgers' circuit

analysis of HREM images revealed that the most common defects present at the interface were either perfect Lomer edge dislocations with a Burgers' vector of (1/2)***a***<110> along the interface, or perfect 60° dislocations with Burgers' vector of the same length but inclined at an angle of 45° to the interface [6]. Aberration-corrected images of these two types of defects are shown below.

The separation between interfacial defects was found to decrease as the lattice mismatch was further increased. For the ZnTe(001)/GaAs(001) heterostructures (mismatch ~7.38%), the interfacial defects were observed to be pseudo-periodic with average separations of ~5.5nm. Figure 4 shows a representative region of the ZnTe/GaAs interface, with the positions of misfit dislocations indicated by arrows. Burgers' circuit analysis of individual defects was again used to identify the dislocation type, although digital image processing provided a far more efficient approach for analyzing larger fields of view. Thus, similar lattice-fringe images were digitized, processed by Fast Fourier Transform (FFT), and then filtered by selecting specific (111) diffraction spots for inverse FFT. The location *and* type of the interfacial misfit dislocations could then be easily determined: perfect Lomer edge dislocations were identified when two corresponding (111) planes terminated at the same location, whereas 60° dislocations were present when a single (111) plane terminated at the interface [5]. Measurements showed that the ratio of Lomer dislocations to the total number of dislocations for the ZnTe/GaAs sample was about 39%. Further analysis taking the type of defect into account also indicated that the residual interfacial strain was ~0.1% for this sample, so that the interface could thus be considered as being relaxed to within experimental error [6].

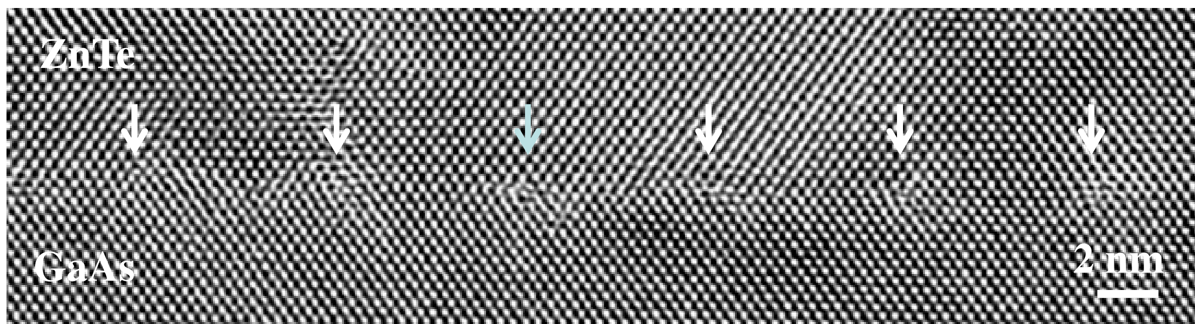

Figure 4. High-resolution lattice-fringe image showing array of dislocations (pseudo-periodic) accommodating the misfit at ZnTe(001)/GaAs(001) interface [6].

3.2. Aberration-corrected electron microscopy

The recent emergence of multiple techniques for aberration correction using either (on-line) hardware or (off-line) software approaches, augmented by improved beam coherence and improved mechanical and electrical stabilities, has enabled microscope information limits to be pushed routinely to beyond the 1 Å resolution barrier [7]. This revolution in aberration correction has dramatically altered the landscape for advanced materials research by making it straightforward to achieve atomic-resolution imaging on a regular basis from many different types of crystalline materials, including metals, oxides and semiconductors. For the specific cases of elemental and compound semiconductors observed in the most commonly used <110> orientation, it then becomes possible to resolve the projections of individual atomic columns, which are often referred to as 'dumbbells' [8]. As an illustrative example, Fig. 5 compares HAADF and BF images, recorded simultaneously with a probe-corrected STEM, which show the interface region of the ZnTe(001)/InP(001) heterostructure mentioned earlier. Individual atomic columns appear with white contrast in the ("Z-contrast") HAADF image, while they are visible with dark contrast in the BF image. The insets show line traces across several In-P dumbbells. From inspection, it is clear that the separate In and P atomic columns which are separated by 0.146nm are well-resolved in both detector geometries despite the considerable difference in their atomic numbers.

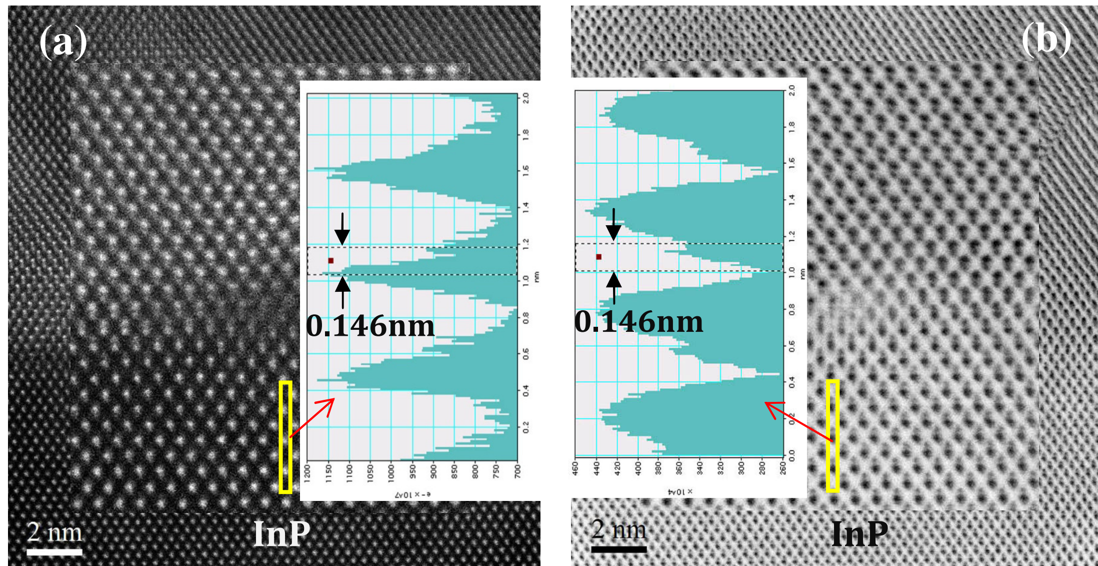

Figure 5. Aberration-corrected STEM images of ZnTe/InP(001) interface: (a) HAADF image (90~170mrad); (b) BF image (0~22mrad). Inset profiles show resolved In-P dumbbells in both cases.

Aberration-corrected imaging is already being widely used although compound semiconductors have so far attracted relatively less attention [8]. However, it should be abundantly clear that the enhanced capability for imaging individual atomic columns should enable improved insights about defect microstructure and structural properties to be obtained, as recently demonstrated, for example, in AC-STEM studies of CdTe solar cells [9]. As another illustration of these possibilities, Fig. 6 shows aberration-corrected STEM images of the two most common types of interfacial defects observed at the ZnTe/InP(001) interface, together with the corresponding Burgers' circuit analysis. By inspection, it seems that the BF image displays clearer 'dumbbell' contrast but neither image shows well-resolved structure at the dislocation cores, which is perhaps attributable to e-beam damage during observation.

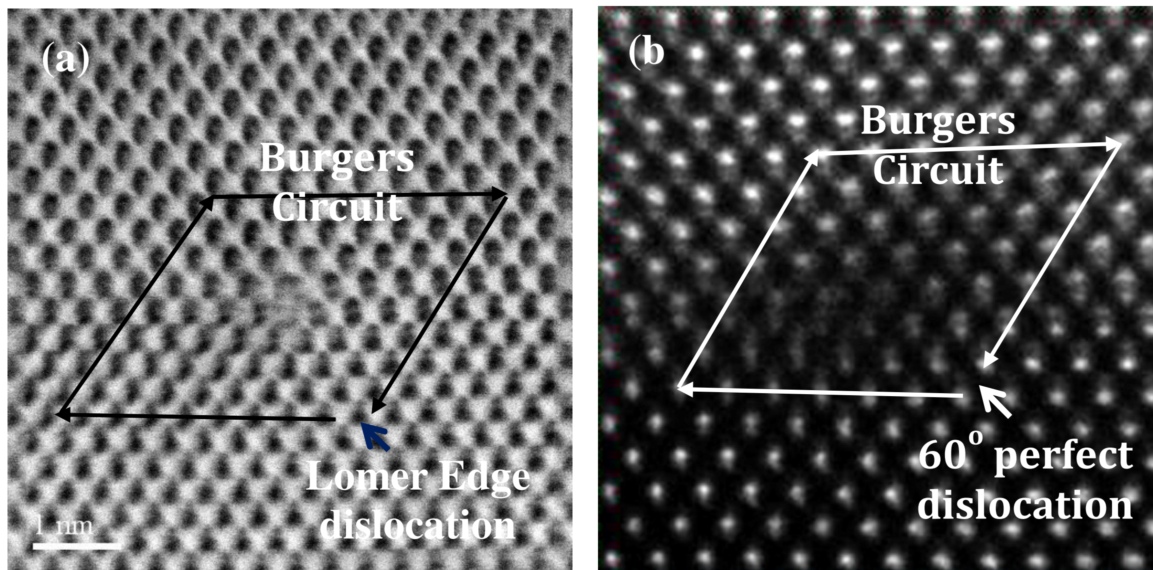

Figure 6. Aberration-corrected STEM images of ZnTe/InP(001) interface: (a) BF image showing Burgers' circuit analysis for Lomer edge dislocation; (b) HAADF image showing Burgers' circuit for perfect 60° misfit dislocation. Individual atomic columns have better visibility in BF image.

Figure 7 compares AC-STEM HAADF and BF images of a perfect Lomer edge dislocation as observed at the ZnTe/GaAs(001) interface. Both images clearly show the 'dumbbell' structure for each material, while line traces of the GaAs region (not shown here) enable the separate Ga and As atomic columns to be identified on the basis of their intensity. The atomic structure of the dislocation core is, however, unclear and further observations are needed to establish whether this apparent disorder has been caused by sample preparation artifacts and/or electron-beam irradiation or whether misfit dislocations at such heterovalent semiconductor interfaces are intrinsically likely to be dissociated.

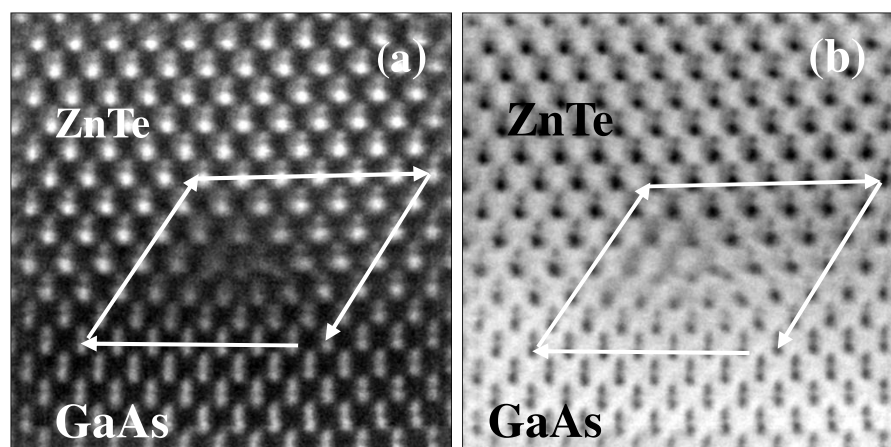

Figure 7. Aberration-corrected STEM images showing Burgers' circuit analysis identifying perfect Lomer edge dislocation at ZnTe/GaAs(001) interface. Individual atomic columns are clearly visible in both images and both materials except close to the dislocation core.

4. Conclusions

Atomic-resolution imaging with the electron microscope has been demonstrated to play a valuable role in characterizing the defect microstructure of zincblende semiconductors. The increased resolving power of aberration-corrected instruments offers further scope for detailed structural investigations at the level of individual atomic columns. Complementary theoretical modeling is still sorely needed to determine the equilibrium structure for heterovalent semiconductor interfaces [9].

References

[1] Zhang YH, Wu SN, Ding D, Yu SQ and Johnson SR 2008 *33rd. IEEE PVSC* pp.1-5

[2] Fan J, Ouyang L, Liu X, Furdyna JK, Smith DJ and Zhang YH 2011 *J. Cryst. Growth* **323** 127

[3] Wang CZ, Smith DJ, Tobin S, Parados T, Zhao J, Chang Y and Sivananthan S 2006 *J. Vac. Sci. Technol.* A **24** 995

[4] Zhang X, Wang S, Ding D, Liu X, Tan JH, Furdyna JK, Zhang YH and Smith DJ 2009 *J. Electron. Mater.* 38 1558

[5] Chai J, Noriega OC, Dinan JH, Smith C, Chau N, Pena J, Dedigama A, Kim JJ, Smith DJ and Myers TH 2013 *J. Electron. Maters.* (in press).

[6] Ouyang L, Fan J, Wang S, Lu X, Zhang YH, Liu X, Furdyna JK and Smith DJ 2011 *J. Cryst. Growth* **330** 30

[7] Smith DJ 2008 *Microsc. Microanal.* **14** 2

[8] Smith DJ, Aoki T, Mardinly J, Zhou L and McCartney MR 2013 *Microscopy* **62** S65

[9] Li C, Poplawsky J, Wu Y, Lupini AR, Mouti A, Leonard DN, Paudel N, Jones K, Yin W, Al-Jassim M, Yan Y and Pennycook SJ 2013 *Ultramicroscopy* (in press)

[10] We acknowledge use of facilities in the John M. Cowley Center for High Resolution Electron Microscopy at Arizona State University. Acquisition of the JEM-ARM200F was supported by NSF DMR-0820196, and the work at Notre Dame was supported by NSF ECC1002072.